ELSEVIER

Colloids and Surfaces A: Physicochem. Eng. Aspects 222 (2003) 15–25

COLLOIDS AND SURFACES A

www.elsevier.com/locate/colsurfa

Particle deposition at electrostatically heterogeneous surfaces

Zbigniew Adamczyk *, Barbara Siwek, Paweł Weroński, Katarzyna Jaszczółt

Institute of Catalysis and Surface Chemistry, Polish Academy of Sciences, ul. Niezapominajek 8, 30-239 Kraków, Poland

Abstract

Irreversible adsorption of negatively charged polystyrene latex particles (averaged diameter 0.9 μm) at heterogeneous surfaces was studied experimentally. The substrate of controlled heterogeneity was produced by covering freshly cleaved mica sheets by positively charged polystyrene latex (averaged diameter of 0.47 μm) to a desired surface coverage. Positive latex deposition was carried out under convection and diffusion-controlled transport conditions and the coverage (defined as heterogeneity degree) was determined by direct particle counting using the optical and electron microscopy. Deposition kinetics of larger latex particles at heterogeneous surfaces produced in this way was studied by using the direct optical microscope observations in the impinging-jet and diffusion cells. It was demonstrated that the initial adsorption rate under the convection-controlled transport attained the limiting value pertinent to homogeneous surfaces for heterogeneity degree of a few per cent. This effect was even more pronounced for diffusion-controlled transport conditions. This behaviour was quantitatively interpreted in terms of the theoretical model considering the coupling between surface and bulk transport of particles. Similarly, the experimental results obtained for higher surface coverage of latex (long adsorption times) were in a good agreement with the generalised random sequential adsorption (RSA) model.

Keywords: Adsorption of colloids; Colloid adsorption; Deposition of particles; Heterogeneous surfaces; Irreversible adsorption; Kinetics of particle adsorption; Latex particle deposition

1. Introduction

Adsorption and deposition (irreversible adsorption) of colloids, proteins and other bio-materials on solid/liquid interfaces is of large significance for many processes such as filtration, membrane filtration, paper-making, chromatography, thrombosis, separation of proteins, bacteria, viruses, enzymes, pathological cells, etc. The effectiveness of these processes is often enhanced by the use of coupling agents bound to interfaces, e.g. polyelectrolytes [1–5] or self assembled monolayers of organosulphur compounds on gold and other metals [6,7]. In biomedical applications special proteins (ligands) attached to the surface are applied for a selective binding of a desired solute from protein mixtures as is the case in the affinity chromatography [8].

Similarly, experimental studies on colloid particle adsorption have often been carried out for surfaces modified by adsorption of polymers, surfactants or chemical coupling agents (silanes),

* Corresponding author. Tel.: +48-12-425-2841; fax: +48-12-425-1923.

E-mail address: ncadamcz@cyf-kr.edu.pl (Z. Adamczyk).

0927-7757/03/$ - see front matter
doi:10.1016/S0927-7757(03)00218-8

which change the natural surface charge of substrate surfaces [9,10]. This is often the case with natural mica used as molecularly smooth substrate in many particle deposition studies [11]. Another important example is adsorption of ionic species, e.g. heavy metal ions, at oxide surfaces bearing various sites, usually characterised by a wide spectrum of binding energy [12]. As demonstrated in [13,14], ion adsorption leads to formation of a nonuniform distribution of charges over glass beads used for filtration experiments in the packed bed columns. A characteristic feature of all these processes is that ion, particle or protein adsorption occurs at surfaces, which are inherently heterogeneous.

Despite significance of particle adsorption at such surfaces, this subject has been little studied experimentally. The existing results were obtained for polystyrene latex adsorbing at mica under the convection-dominated transport conditions in the impinging-jet cells [15,16]. Similarly, Elimelech et al. [12,13] have shown experimentally that a significant increase in the initial deposition rate of latex colloid occurred for substrates (glass beads) characterised by heterogeneous charge distribution.

Up to our knowledge, no results have been reported in the literature for the important case of diffusion-controlled adsorption pertinent to protein and biocolloid systems.

The goal of this paper is to determine experimentally colloid particle adsorption at heterogeneous surfaces under the purely diffusion transport conditions. Besides direct applications for predicting biocolloid adsorption at heterogeneous surfaces, the results obtained can be exploited for elucidating the mechanism and modelling the kinetics of molecular adsorption as well, especially to determine the range of validity of the Langmuirian model.

2. Experimental

Particle deposition experiments have been carried out using the direct microscope observation method in the diffusion cell shown in Fig. 1. The main part of the cell was a Teflon container of

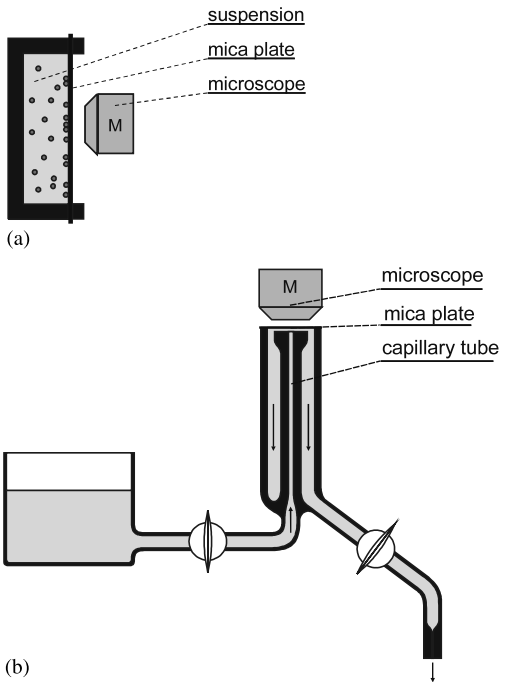

Fig. 1. The experimental cells used for measurements of latex deposition at heterogeneous surfaces, part "a": the diffusion cell, part "b": the impinging-jet cell.

dimensions $1.5 \times 2.5 \times 8$ cm (height) with an rectangular window of the dimension of 2×6 cm made of the mica sheet, used as the substrate for particle adsorption. The cell was used previously in studies of particle adsorption at homogeneous surfaces [17,18]. A similar parallel-plate channel arrangement of the cell was exploited for adsorbing colloid particles in the streaming potential measurements for heterogeneous surfaces [19]. The cell was fixed to the optical microscope stage (Nikon) that was attached to a special metal table, which could be inclined (rotated) by an angle reaching 90°. In the latter case, the microscope was oriented horizontally with the objective perpendicular to the substrate surface (see Fig. 1). In this arrangement gravity was directed parallel to the mica surface eliminating effectively the particle sedimentation effect. Deposition kinetics and particle distribution over the substrate was followed in situ using a long-distance objective coupled with a CCD camera (Hamamatsu C-3077) and a image analysing system.

Some reference deposition experiments also have been carried out in the impinging-jet cell used extensively before for similar studies [9–11]. This cell is shown schematically in Fig. 1 as well. Because of the hydrostatic pressure difference the particle suspension was driven through a circular capillary of the radius $R = 0.1$ cm, impinged against a perpendicularly oriented mica plate, and left the cell through the external tubing. After use, the suspension was discarded. The volumetric flow rate in the cell Q was regulated by changing the level of the outlet tubing. This allowed one to regulate the flow Reynolds number $Re = Q/\pi Rv$ within broad limits (where v is the kinematic viscosity of the suspension). Because of the under-pressure prevailing in the cell, the mica plate was held fixed to the external tubing without using any adhesive that reduced the possibility of cell contamination during the measurements.

Adsorbed particles were observed in situ under an optical microscope (Leitz, Germany, dark-field illumination) coupled with a CCD camera and an image processor.

Two samples of polystyrene latex were used in our deposition kinetic studies. The negatively charged latex was synthesised according to he polymerisation procedure described in [20] using a persulphate initiator. The concentrated stock samples obtained from the polymerisation were purified by steam distillation and prolonged membrane filtration according to the procedure described previously [9,10]. Particle size distribution and concentration in the dilute samples used in experiments were determined by the Coulter-Counter and by laser diffractometer with an accuracy of a few percent. The averaged size of the negative latex used in our experiments was 0.9 μm with standard deviation of 0.06 μm. The positively charged latex suspension (used for modelling adsorption sites) was produced and cleaned according to a similar procedure with the azonitrile initiator in place of the persulphate initiator. The averaged diameter of the latex was 0.47 μm with the standard deviation of 0.04 μm as determined by a laser difractometer. Zeta potential of latex samples was determined by the Brookhaven zetasizer. For $I = 10^{-3}$ M KCl and pH 5.5 (particle deposition experimental conditions) zeta potential of the negative latex was −50 mV, whereas for the positive latex 50 mV, respectively.

As mentioned, the adsorbing surface was prepared of mica provided by Mica & Micanite Supplies Ltd. England. Zeta potential of this mica was determined by the streaming potential method in the plane-parallel channel cell [19]. For the above experimental conditions zeta potential on mica was −80 mV.

The experimental procedure was the following: a freshly cleaved mica sheet was cut to the appropriate size and mounted into the cell's window without using any adhesive. Then the positive latex suspension was carefully poured into the cell. Particle deposition was carried out for a desired time (typically 0.5–1 h) until the prescribed surface concentration of particles was attained. The surface concentration was determined by a direct microscope counting over statistically chosen areas. The total number of particles counted was about 1000, which ensured a relative precision of coverage determination better than 3%. For sake of convenience the surface concentration of particles was expressed as the dimensionless coverage $\Theta_s = \pi a_s^2 \langle N_s \rangle$ (where N_s is the average surface concentration of adsorbed smaller particles and as is their averaged radius). In our experiments Θ_s varied between 0 and 0.1. After preparing the heterogeneous substrate, the positive latex suspension was replaced by 10^{-3} M KCl solution and then by the negative latex suspension and the particle deposition run was continued for a period reaching 48 h. The bulk suspension concentration of the negative latex n_b was typically 10^9 cm^{-3}. Images of adsorbed particles were collected in situ at prescribed time intervals. Adsorption kinetics of latex was followed by determining the averaged surface concentration $\langle N_p \rangle$ of particles found on these images as a function of the time t. For obtaining a single point on the kinetic curve 100–500 particles were counted over statistically chosen areas having typical dimensions of 100 per 100 μm. The dimensionless surface coverage of adsorbed larger particles was expressed as $\Theta_p = \pi a_p^2 \langle N_p \rangle$, where N_p is the surface concentration of larger-particles and a_p is their average radius. After completing the deposition run the latex suspension was carefully washed out by water and mica

surface covered with particles was examined again under wet conditions. This procedure was selected because we have observed that drying up of the sample induced significant structure changes in the particle monolayer.

It was proven in separate experiments that particle adsorption was perfectly irreversible and localised. No lateral motion or particle desorption was observed when rinsing particle monolayers with electrolyte (10^{-3} KCl) in situ by a prolonged period of time.

3. Results and discussion

In order to select appropriate conditions for controlled preparation of heterogeneous mica (covered by positive latex particles) a series of preliminary kinetic measurements for the positive latex was performed under both convection and diffusion-controlled transport modes. A typical kinetic run measured in the impinging-jet cell ($Re = 4$, bulk suspension concentration $n_b = 1.6 \times 10^9$ cm^{-3}) is shown in Fig. 2(a). As can be noticed, for the initial stage of latex adsorption at mica, the dependence of Θ_s on the adsorption time t was linear. This is in a quantitative agreement with theoretical predictions shown by the solid line in Fig. 2(a). The theoretical result has been derived by a numerical solution of the governing mass transfer equation according to the procedure discussed extensively elsewhere [11,21]. It was demonstrated by a throughout variance analysis that latex particle distributions were statistically uniform with no tendency to clustering as is often the case for mono-layers dried before microscope observation. The kinetic curve shown in Fig. 2(a) enabled one to fully control particle coverage Θ_s via the deposition time. However, the real coverage was determined quantitatively, as mentioned above, by direct counting of the number of adsorbed particles.

Analogous results have been obtained in the case of diffusion-controlled transport conditions, see Fig. 2(b). As can be observed the coverage Θ_s increased in this case linearly with the square root of the deposition time t, in accordance with the formula

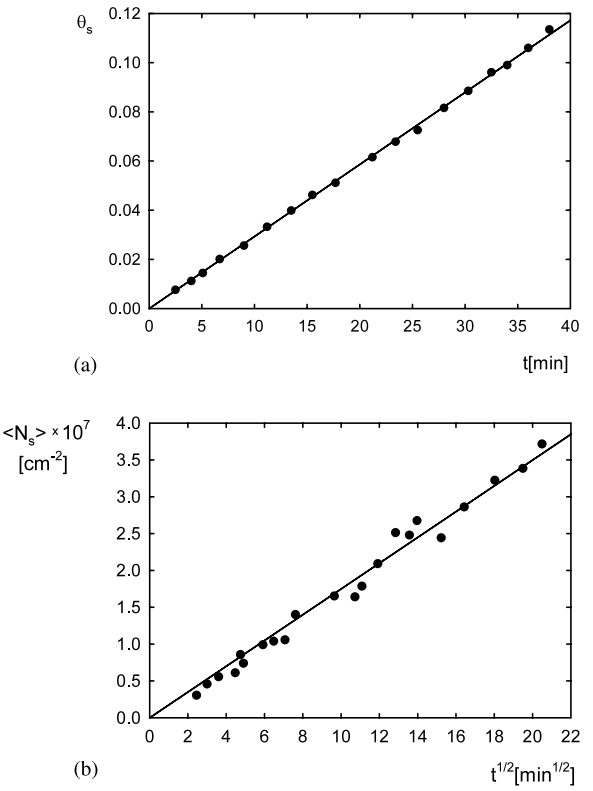

Fig. 2. Initial adsorption kinetics of positive latex (averaged diameter 0.47 μm) at bare mica, $I = 10^{-3}$ M, part "a": the impinging-jet cell, $Re = 4$, $n_b = 1.6 \times 10^9$ cm^{-3}; part "b": the diffusion cell $n_b = 2.0 \times 10^9$ cm^{-3}. The solid lines denote the theoretical predictions derived by numerical solutions of the governing transport equation for part "a" and from Eq. (1), for part "b".

$$\Theta_s = 2\pi a_s^2 \sqrt{\frac{D_\infty t}{\pi}}\, n_b \tag{1}$$

where $D_\infty = kT/6\pi\eta a_s$ is the diffusion coefficient of the particle in the bulk (k is the Boltzmann constant, T is the absolute temperature and η is the dynamic viscosity of the suspension). Eq. (1) also can be expressed in the dimensional form as

$$\langle N_s \rangle = 2\sqrt{\frac{D_\infty t}{\pi}}\, n_b \tag{2}$$

Because both $\langle N_s \rangle$ (the averaged number of particles per unit area) and n_b can be determined experimentally (the latter quantity via the direct dry weight method), Eq. (2) enables one to

calculate the diffusion coefficient. By knowing the temperature and the viscosity one can determine particle size. It was found in this way that $2a_s = 0.47$ μm in agreement with the value obtained from the difractometer.

Having established the conditions for obtaining the desired coverage Θ_s a series of deposition experiments of larger (negative) latex at heterogeneous mica was performed. It was first demonstrated that no measurable deposition of negative latex was observed in the case of bare mica, hence, latex particle adsorption occurred if $\Theta_s > 0$ only. Moreover, it was proven experimentally that in the case of $\Theta_s > 0$ larger particles adsorbed at heterogeneities (smaller particles) only. One can assume, therefore, that the deposition procedure of the smaller latex did not contaminated mica surface by low molecular weight species. This is confirmed by the micrographs shown in Fig. 3(a, b). In Fig. 3(a) a typical configuration of negative latex particles adsorbed at the heterogeneous surface under the convection-controlled transport ($Re = 4$, $\Theta_s = 0.13$, $\Theta_p = 0.12$) is shown. On the other hand, in Fig. 3(b) the configuration observed under diffusion-controlled transport is presented ($\Theta_s = 0.12$, $\Theta_p = 0.11$). The apparent differences in particle size are caused by different illumination conditions prevailing in the impinging-jet and the diffusion cells.

A quantitative characterisation of particle distributions can be attained in terms of the pair correlation function $g(r)$ (referred often to as the radial distribution function) [10,22]. The function was calculated from the constitutive dependence

$$g(r) = \frac{\pi a_p^2}{\Theta_p} \left\langle \frac{\Delta N_p}{2\pi r \Delta r} \right\rangle \tag{3}$$

where $\langle\ \rangle$ means the ensemble average and N_p is the number of particles adsorbed within the ring $2\pi r\ \Delta r$ drawn around a central particle. The function can be interpreted as an averaged probability of finding a particle at the distance r from another particle (with the centre located at $r = 0$) normalised to the uniform probability at large distances. As can be seen in Fig. 3(a, b), the $g(r)$ function determined experimentally for larger particles under both convection and diffusion-controlled transport conditions are similar. In both cases the experimental results are well reflected by the theoretical data derived from numerical simulations reported elsewhere [22]. A characteristic feature of the $g(r)$ function shown in Fig. 3(a, b) is that it does not vanish for $r/a_p < 2$. The finite value of $g(r)$ observed in this range spectacularly confirms the fact that particles are adsorbed in various planes due to the finite size of the adsorption sites. This means that their projections on the adsorption plane can overlap. This apparent overlapping effect is analogous to previously observed for adsorption at homogeneous interfaces of polydisperse particles [23].

Besides studying the structural aspects the main goal of this work was determining adsorption kinetics at heterogeneous surfaces as a function of the heterogeneity degree identified in our case with the coverage of smaller particles Θ_s. Some typical kinetic runs evaluated for the initial stage of adsorption when blocking effects remained negligible are shown in Fig. 4(a) for the convection-controlled transport and in Fig. 4(b) for the diffusion-controlled transport. As one can notice in Fig. 4(a), the dependency of latex coverage Θ_p on the adsorption time t was linear with the slope increasing abruptly with the heterogeneity degree Θ_s. As can be observed, for Θ_s as low as a few per cent, particle adsorption rate at heterogeneous surfaces attained the limiting value pertinent to uniform surfaces (shown by dashed line in Fig. 4(a)). The linearity of the kinetic runs shown in Fig. 4(a) enables one to calculate the initial flux of particles (initial adsorption rate) using the definition

$$|j_0| = \frac{1}{\pi a_p^2} \frac{\Delta \Theta_p}{\Delta t} \tag{4}$$

where $\Delta\Theta_p/\Delta t$ is the slope of the experimental kinetic run fitted by linear regression lines. It was also shown in separate runs that the initial flux was proportional to the bulk suspension concentration n_b, which indicates that larger particle adsorption was indeed a linear process for the entire range of times studied. This fact enabled one to increase the accuracy of experimental determination of the initial flux since averages from many

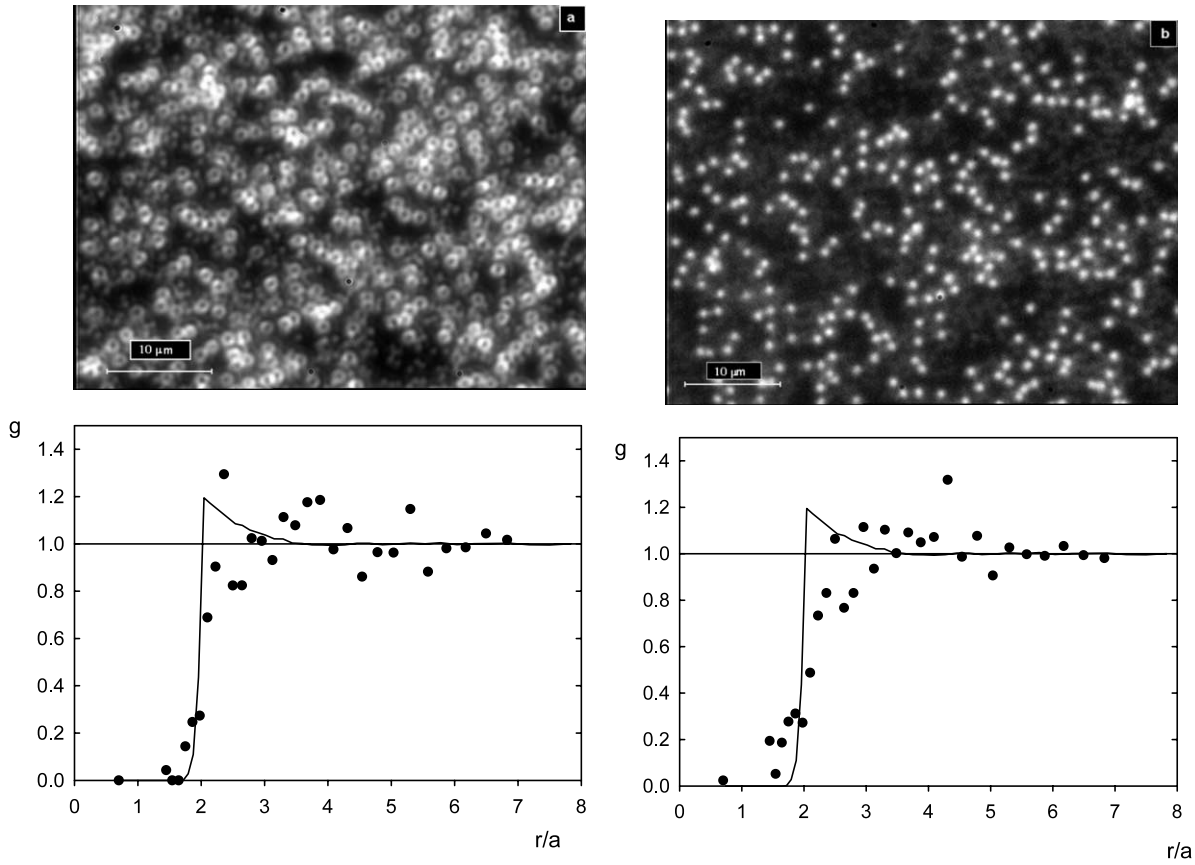

Fig. 3. Micrograph of larger polystyrene latex particles adsorbed at heterogeneous surfaces (mica pre-covered by smaller-sized latex) and the corresponding pair correlation functions $g(r/a)$, part "a", the impinging-jet cell, $Re = 4$, $\Theta_s = 0.127$, $\Theta_p = 0.123$, part "b", the diffusion cell, $\Theta_s = 0.122$, $\Theta_p = 0.107$.

kinetic runs performed for various n_b could be taken. It is, therefore, advantageous to express the initial flux in the reduced form $-j_0(\Theta_s)/n_b = k_b(\Theta_s)$, where $k_b(\Theta_s)$ is the mass transfer rate constant. We determined experimentally the dependence of the reduced flux on the heterogeneity degree Θ_s. It was found that the maximum value of $|j_0(\Theta_s)/n_b|$ approached 9.7×10^{-6} cm s^{-1} for $Re = 4$ and $I = 10^{-3}$ M. This is slightly above the theoretical value pertinent to uniform surfaces equal $j_{mx} = 8.9 \times 10^{-6}$ cm s^{-1}, measured for homogeneous surfaces. Similar results were obtained for other Re number as well. The slight positive deviation from the theoretical predictions can probably be attributed to the interception effect discussed in [11].

Analogous behaviour was observed for the diffusion-controlled transport, see Fig. 4(b). In this case, however, Θ_p was expressed as a function of the square root of the adsorption time. As can be seen, the experimental kinetic runs became approximately linear after a short transition time with the slope increasing abruptly with the heterogeneity degree. Practically, for $\Theta_s > 0.05$ the kinetic of particle adsorption at heterogeneous surfaces became identical with the kinetics pertinent to homogeneous surfaces. Hence, for heterogeneity degree exceeding a few per cent, the reduced particle flux attained the limiting value characteristic for uniform surfaces

$$j_{mx}(t) = -\sqrt{\frac{D_\infty}{\pi t}}\, n_b = k_b(t) n_b \tag{5}$$

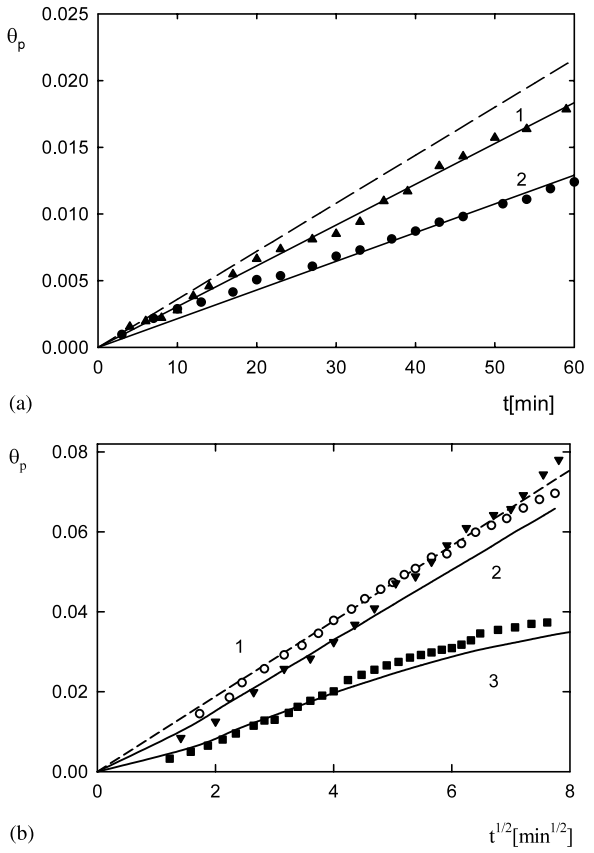

Fig. 4. Initial adsorption kinetics of larger negative latex (average diameter 0.9 μm) at heterogeneous surfaces (mica covered by positive latex), part "a": the impinging-jet cell, $Re = 4$, $n_b = 1.06 \times 10^8$ cm^{-3}; (1) $\Theta_s = 0.032$; (2) $\Theta_s = 0.018$. The solid lines denote the theoretical results calculated by integrating Eq. (10) and the dashed line represents the theoretical results predicted for homogeneous surfaces, part "b", the diffusion cell, (1) $\Theta_s = 0.10$; (2) $\Theta_s = 0.042$; (3) $\Theta_s = 0.0068$. The continuous lines denote the theoretical results calculated by numerical solution of the diffusion equation with the boundary condition, Eq. (20) and the dashed line represents the limiting solution for homogeneous surfaces calculated from Eq. (1).

The limiting flux for uniform surfaces, $j_{mx}(t)$ is an important parameter because it can be used as a scaling variable for expressing the experimental results in the reduced form $\bar{j} = j(\Theta_s, t)/j_{mx}(t)$. This form of presentation of experimental results is advantageous for their theoretical analysis as demonstrated in [7,8]. In Fig. 5 the experimentally determined dependence of the scaled flux $\bar{j} = j(\Theta_s, t)/j_{mx}(t)$ on Θ_s is plotted. As can be observed the reduced flux increased abruptly with Θ_s approaching the limiting values for Θ_s of a few percents. These experimental evidences suggest that the kinetics of particle adsorption at heterogeneous surfaces in this limit can well be predicted by the well-known results pertinent to uniform surfaces [11,22]. This has a considerable significance since many of the known theoretical and experimental data for uniform surfaces can directly be transferred to heterogeneous system adsorption.

A quantitative interpretation of the experimentally found dependence of $\bar{j}$ on Θ_s can be attained in terms of the theoretical random sequential adsorption (RSA) model elaborated in [22–24]. The basic assumption of this theoretical approach was that the colloid particles can only be adsorbed upon touching the site. Physically this corresponds to the situation when particles become irreversibly bound to the sites as a result of short-ranged attractive interactions of electrostatic or chemical nature. Furthermore, particle adsorption was assumed irreversible and localised, which means that particle position at the site remained fixed during the entire process. It was demonstrated by performing extensive numerical simulations within the framework of the RSA model [22] that the initial adsorption probability, when there are no adsorbed particles except heterogeneities, can well

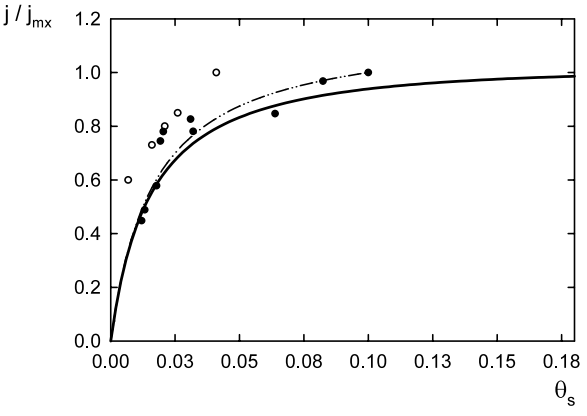

Fig. 5. The dependence of the normalised flux of particles $\bar{j} = j/j_{mx}$ on Θ_s. The full points denote the experimental results obtained for $Re = 4$, $I = 10^{-3}$ M, $\lambda = 1.95$, the empty points represent the results obtained in the diffusion cell, the solid line represents the theoretical results derived from Eq. (10) for $K = 8$ and the dashed line shows the results calculated from Eq. (11).

be approximated by the analytical formula

$$p_0(\Theta_s) = 1 - (1 - \Theta_s)e^{-\frac{(4\lambda-1)\Theta_s}{1-\Theta_s} - \left[\frac{(2\sqrt{\lambda}-1)\Theta_s}{1-\Theta_s}\right]^2} \quad (6)$$

where $\lambda = a_p/a_s$ is the particle size ratio, being a parameter of a crucial importance. For $\lambda\Theta_s << 1$, Eq. (6) reduces to the simple form

$$p_0(\Theta_s) = 4\lambda\Theta_s \quad (7)$$

Knowing p_0 one can express the flux of particles in the adsorption layer in the form [25,26]

$$-j(\Theta_s) = j_a = k_a n_b p_0(\Theta_s) \quad (8)$$

where j_a is the reference flux in the adsorption layer, k_a is the adsorption rate constant calculated as [25,26]

$$k_a = \left[\int_{\delta_m}^{\delta_a} \frac{dh}{D(h)}\right]^{-1} \quad (9)$$

where δ_m is the minimum distance between the adsorbing particle and the interface, δ_a is the thickness of the heterogeneous particle layer, h is the surface to surface distance of the particle and the interface and $D(h)$ is the particle diffusion coefficient depending on the distance from the interface h.

In the general case, Eq. (8) is to be used as the boundary condition for the bulk transport equation [25]. In the case of convection-controlled transport after a short transition time of the order of a second the flux becomes quasi-stationary [11]. Then, the solution of the bulk transport equation with the boundary conditions, Eq. (8) can be expressed in the analytical form [15]

$$\bar{j} = \frac{1}{\pi a_p^2 |j_{mx}|}\frac{d\Theta_p}{dt} = \frac{Kp_0(\Theta_s)}{1 + (K-1)p_0(\Theta_s)} \quad (10)$$

where $K = j_a/j_{mx} = k_a n_b/k_b n_b$.

A useful analytical expression can be derived if $\lambda\Theta_s \ll 1$. Then, Eq. (10) becomes

$$\bar{j} = \frac{4\lambda K\Theta_s}{1 + 4\lambda(K-1)\Theta_s} \quad (11)$$

The theoretical results stemming from Eqs. (10) and (11) are also shown in Fig. 5. The relevant parameters for our experimental conditions were $\lambda = 1.95$ (particle size ratio) and $K = 8$. The latter value was calculated by assuming the thickness of the adsorption layer δ_a equal to the diameter of smaller latex particles (heterogeneities) and $k_b = 8.9 \times 10^{-6}$ cm s^{-1} (this is the measured value for $Re = 4$). As one can observed in Fig. 5, Eq. (10) reflect well the experimental results for $\Theta_s < 0.02$. The positive deviation of the experimental data from the theoretical predictions observed for higher coverage can probably be attributed to the interception effect [11]. As expected, Eq. (11) also gives a satisfactory agreement with the experimental data for $\Theta_s < 0.05$. This has a considerable practical significance in view of the simplicity of these analytical expressions. The agreement between the experimental results and theoretical predictions derived from Eqs. (10) and (11) suggests, therefore, that the model can be useful for a quantitative interpretation of particle deposition kinetics at heterogeneous surfaces. Moreover, this agreement suggests that electrostatic hetero-interactions between the smaller and larger latex particles proved efficient for ensuring an irreversible and localised adsorption. It is interesting to note that these results are very similar to the experimental data obtained under the diffusion-controlled transport conditions (shown by open symbols in Fig. 5). In both cases the scaled flux increases abruptly with the heterogeneity degree Θ_s. This can be interpreted to the fact that after a failed adsorption attempt (at the interface area devoted of heterogeneities) the particle can reach by diffusion another adsorption centre in their vicinity, before it returns to the bulk. The results shown in Fig. 5 for our model system (latex adsorption on latex) can be exploited to predict adsorption kinetics in more complicated systems where direct measurements of adsorption kinetics are not possible, e.g. proteins.

It should be remembered, however, that the above experimental data concerned the initial adsorption stages when larger latex particle accumulation at the surface remained negligible. For higher particle coverage a significant deviation of adsorption kinetics from linearity occurred as a results of the blocking effects studied extensively for uniform surface adsorption [11,26,27]. This can be observed in Fig. 6(a) showing the results

obtained for the convection-controlled transport and in Fig. 6(b) where the results obtained for the diffusion-controlled transport. After an initial linear rise, the coverage of larger particles Θ_p saturated at a value, which strongly increased with the heterogeneity degree Θ_s. A quantitative interpretation of these results is possible in terms of Eq. (8). However, the probability of particle adsorption becomes dependent in this case both on Θ_p and Θ_s. It was demonstrated in [22] by performing extensive numerical simulations that for low Θ_p particle adsorption probability can be approximated by the quasi-Langmuirian expression

$$p(\Theta_s, \Theta_p) = 4\lambda\Theta_s(1-\Theta_p/\lambda^2 n_s\Theta_s)(1-q\Theta_p) = p_0(1-\Theta_p/\Theta_p^{mx}) \quad (12)$$

where n_s is the site multiplicity parameter obtained from simulations and

$$\Theta_p^{mx} = \frac{\lambda^2 n_s\Theta_s}{1+q\lambda^2 n_s\Theta_s} \quad (13)$$

can be treated as the apparent maximum coverage. Eq. (12) remains valid if $\lambda^2 n_s\Theta_s < 0.1$.

On the other hand, for $\lambda^2 n_s\Theta_s > 0.1$ the function $p(\Theta_s, \Theta_p)$ can be expressed as [22]

$$p(\Theta_s, \Theta_p) = p_0(\Theta_s)B(\Theta_p) \quad (14)$$

where $B(\Theta_p)$ is the blocking function pertinent to the RSA model, which can be approximated by the formula [22,28,29]

$$B(\bar{\Theta}_p) = f(\bar{\Theta}_p)(1-\bar{\Theta}_p)^3 \quad (15)$$

where $\bar{\Theta} = \Theta_p/\Theta_p^{\infty}$, Θ_p^{∞} is the jamming coverage known from simulations (for homogeneous surfaces it is equal 0.547), and $f(\bar{\Theta}_p)$ are the low-order polynomials. One of the most accurate interpolation polynomials describing $f(\bar{\Theta}_p)$ has the form [28,29]

$$f(\bar{\Theta}_p) = 1 + 0.812\bar{\Theta}_p + 0.426\bar{\Theta}_p^2 + 0.0716\bar{\Theta}_p^3 \quad (16)$$

Using these expressions the particle flux can be expressed as

$$\bar{j} = \frac{1}{\pi a_p^2|j_{mx}|}\frac{d\Theta_p}{dt} = \frac{Kp(\Theta_s, \Theta_p)}{1+(K-1)p(\Theta_s, \Theta_p)} \quad (17)$$

By integrating Eq. (17) in respect to time one obtains the following kinetic equation.

$$(K-1)\Theta_p + \int_0^{\Theta_p} \frac{d\Theta'}{p(\Theta_s, \Theta_p)} = K\pi a_p^2|j_{mx}|t \quad (18)$$

In the general case the integral appearing in Eq. (18) can be evaluated numerically only. However, for the low coverage regime when $\lambda\Theta_s\ (K-1) \ll 1$, Eq. (18) can be integrated analytically. Using Eq. (12) one can derive the following expression in this case

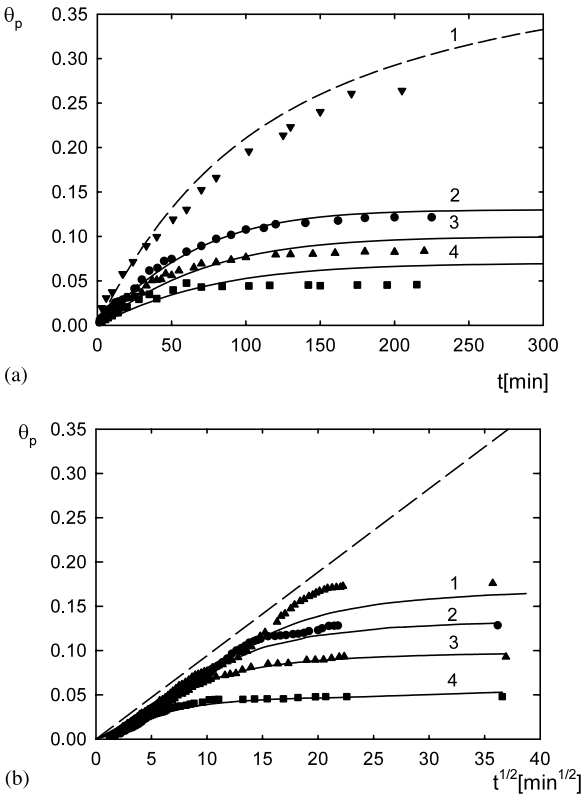

Fig. 6. Adsorption kinetics at heterogeneous surfaces for the nonlinear regimes, part "a" the impinging-jet cell, $Re = 4$, $I = 10^{-3}$ M, (1) $\Theta_s = 0.13$; (2) $\Theta_s = 0.032$; (3) $\Theta_s = 0.019$; (4) $\Theta_s = 0.012$. The solid lines denote the theoretical results calculated from Eq. (19) and the dashed line represents the theoretical results predicted for homogeneous surfaces from Eq. (18), part "b", the diffusion cell, $I = 10^{-3}$ M, (1) $\Theta_s = 0.026$; (2) $\Theta_s = 0.022$; (3) $\Theta_s = 0.017$; (4) $\Theta_s = 0.0068$. The solid lines denote the theoretical results calculated numerically by solving the diffusion equation with the boundary condition, Eq. (20) and the dashed line represents the theoretical results predicted for homogeneous surfaces.

$$\Theta_p = \Theta_p^{mx}\left[1 - e^{-\frac{4\lambda\Theta_s}{\Theta_p^{mx}}K\pi a^2|j_{mx}|t}\right] \quad (19)$$

where Θ_p^{mx} is the apparent saturation coverage given by Eq. (13).

As can be observed in Fig. 6(a) the theoretical results calculated from Eq. (18) described satisfactory the experimental data. The slight deviation appearing at longer adsorption times and $\Theta_s = 0.012$ can probably be attributed to the hydrodynamic scattering effect as demonstrated previously for deposition on homogeneous surfaces [11]. Another explanation would be the finite value of the binding energy between the particle and the site. In consequence, the energy may become insufficient for an irreversible capture of particles under vigorous shearing flows and a small fraction of sites may prove to be inactive in the immobilisation of larger particles. This hypothesis is supported by the fact that for higher Θ_s, when particles adsorb at multiple sites, the agreement between theoretical and experimental data becomes quantitative. In particular, for $\Theta_s > 0.13$ adsorption kinetics at heterogeneous surfaces becomes identical with adsorption at homogeneous surfaces, governed by the RSA model. In this case the theoretical results have been calculated by a numerical integration of Eq. (18) with p given by Eq. (14).

A more complicated situation arises in the case of adsorption under the diffusion-controlled regime because of the inherently non-stationary transport conditions. Hence, in contrast to the convection-controlled transport the thickness of the diffusion boundary layer increases monotonically with time that excludes the possibility of use of Eq. (18) for describing the kinetics of particle adsorption. As a result the theoretical data were obtained by numerical solution of the governing diffusion equation with the following boundary condition at the edge of the adsorption layer δ_a

$$D\frac{\partial n}{\partial h} = k_a n(\delta_a) p_0(\Theta_s) B(\Theta_p) \quad (20)$$

at $h = \delta_a$.

The implicit finite-difference method was used, described in detail elsewhere [25]. As can be seen in Fig. 6(b) the experimental data obtained for various Θ_s are well reflected by the theoretical calculations for the entire range of adsorption time studied (reaching 24 h). The slight positive deviation of experimental points from theoretical predictions observed for higher Θ_s can be probably attributed to the natural convection effects. By extrapolation of the kinetic data to infinite time according to the procedure given in [25] it was found that the maximum coverage for $\Theta_s =$ 0.0068, 0.016, 0.022 and 0.026 was 0.051, 0.10, 0.13 and 0.17, respectively. This agrees well with the theoretical predictions, i.e. 0.053, 0.11, 0.13 and 0.17, respectively. It was also found in separate experiments that for $\Theta_s > 0.1$ particle deposition kinetics and the maximum coverage was identical to the homogeneous surface adsorption. The agreement between experimental and theoretical data demonstrated in Fig. 6(b) suggests that the boundary conditions expressed by Eq. (20) in conjunction with the blocking function derived from simulations adequately describes particle deposition under the diffusion-controlled transport conditions.

.The results shown in Figs. 5 and 6, apparently first of this type in the literature, can be exploited for predicting kinetics of protein and bio-particle adsorption at heterogeneous surfaces.

4. Conclusions

It was demonstrated experimentally that adsorption rate of polystyrene latex on heterogeneous mica can be well reflected by Eq. (11). In accordance with this equation the initial adsorption rate increased abruptly with the heterogeneity degree (coverage of smaller latex Θ_s) attaining the limiting value pertinent to uniform surfaces j_{mx} when $\Theta_s > \frac{1}{4\lambda K}$. This was attributed to the combined effect of geometrical interception, proportional to $4\lambda\Theta_s$ and the coupling with the bulk transport, described by the K parameter. Similar results has been derived for the diffusion-controlled transport conditions.

For higher coverage of adsorbed particles the adsorption kinetics deviated from linearity as a result of blocking effects. This effect was quantitatively accounted for by the theoretical approach based on numerical solutions of the diffusion equation with the non-linear boundary conditions, Eq. (20). It was demonstrated experimentally that the saturation maximum coverage Θ_p increased abruptly with the heterogeneity degree Θ_s, attaining values pertinent to uniform surfaces for Θ_s as low as a few per cent.

Moreover, by determining quantitatively the initial adsorption rate of latex particles of known size used as markers one can detect the presence at interfaces of much smaller objects, for example, adsorbed nanoparticles or proteins.

Acknowledgements

This work was supported by the EC Grant GRD1-2000-26823 and partially by the KBN Grant 7T08B 02821.

References

[1] M.Y. Boluk, T.G.M. van de Ven, Colloids Surf. 46 (1990) 157.
[2] B. Alince, T.G.M. van de Ven, Colloids Surf. A 71 (1993) 105.
[3] T. Serizawa, H. Takashita, M. Akashi, Langmuir 14 (1998) 4088.
[4] J. Schmitt, P. Machtle, D. Eck, H. Mohwald, C.A. Helm, Langmuir 15 (1999) 3256.
[5] K.M. Chen, X. Jiang, L.C. Kimmerling, P.T. Hammond, Langmuir 16 (2000) 7825.
[6] J.J. Skaife, N.L. Abbott, Langmuir 16 (2000) 3529.
[7] J.J. Skaife, N.L. Abbott, Langmuir 17 (2001) 5595.
[8] H.A. Chase, Chem. Eng. Sci. 39 (1984) 1099.
[9] Z. Adamczyk, M. Zembala, B. Siwek, J. Czarnecki, J. Colloid Interf. Sci. 110 (1986) 188.
[10] Z. Adamczyk, M. Zembala, B. Siwek, P. Warszyński, J. Colloid Interf. Sci. 140 (1990) 123.
[11] Z. Adamczyk, B. Siwek, M. Zembala, P. Belouschek, Adv. Colloid Interf. Sci. 48 (1994) 151.
[12] W. Rudziński, R. Charmas, S. Partyka, F. Thomas, J.Y. Bottero, Langmuir 8 (1992) 1154.
[13] M. Elimelech, C.R. O'Melia, Langmuir 6 (1990) 1153.
[14] L. Song, P.R. Johnson, M. Elimelech, Environ. Sci. Technol. 28 (1994) 1164.
[15] Z. Adamczyk, B. Siwek, E. Musiał, Langmuir 17 (2001) 4529.
[16] Z. Adamczyk, B. Siwek, P. Weroński, E. Musiał, Appl. Surf. Sci. 196 (2002) 250.
[17] Z. Adamczyk, L. Szyk-Warszyńska, B. Siwek, P. Weroński, J. Chem. Phys. 113 (2000) 11336.
[18] Z. Adamczyk, L. Szyk, Langmuir 16 (2000) 5730.
[19] M. Zembala, Z. Adamczyk, Langmuir 16 (2000) 1593.
[20] J.W. Goodwin, J. Hearn, C.C. Ho, R.H. Ottewill, Colloid Polym. Sci. 252 (1974) 464.
[21] Z. Adamczyk, M. Zembala, B. Siwek, P. Warszyński, J. Colloid Interf. Sci. 242 (2001) 14.
[22] Z. Adamczyk, P. Weroński, E. Musiał, J. Colloid Interf. Sci. 248 (2002) 67.
[23] Z. Adamczyk, B. Siwek, M. Zembala, P. Weroński, J. Colloid Interf. Sci. 185 (1997) 236.
[24] Z. Adamczyk, B. Senger, J.C. Voegel, P. Schaaf, J. Chem. Phys. 110 (1999) 3118.
[25] Z. Adamczyk, J. Colloid Interf. Sci. 229 (2000) 477.
[26] Z. Adamczyk, Irreversible adsorption of particles, in: J. Toth (Ed.), Adsorption: Theory, Modelling and Analysis, Marcel-Dekker, New York, 2002, pp. 251–374 (Chapter 5).
[27] Z. Adamczyk, B. Siwek, M. Zembala, J. Colloid Interf. Sci. 151 (1992) 351.
[28] P. Schaaf, J. Talbot, J. Chem. Phys. 91 (1989) 4401.
[29] B. Senger, J.C. Voegel, P. Schaaf, Colloids Surf. A. 165 (2000) 255.